Supporting Information

Mishra et al. 10.1073/pnas.1709079114

SI Text

Plasmids and Yeast Strains Construction

All yeast strains and plasmids are listed in Tables S1 and S2, respectively. Standard methods were used for yeast strain construction and molecular biology. Yeast strains are derivatives of BY4741 (1). Gene fusions were generated by homologous recombination-based replacement of the endogenous gene, and expressed from their endogenous promoter unless indicated. Strains for all experiments were grown in synthetic-complete–based media (0.17% Yeast nitrogen base, 2% glucose, 0.5% NH_4 sulfate and amino acids) or yeast extract pentose dextrose (YPD) media. Where indicated, cells were arrested in S phase by adding 200 mM hydroxyurea for 2 h. Cercosporamide (Merck), LatB (Enzo Life Sciences), and 1NaPP1 (1-Naphthyl-PP1; Tocris Bioscience) were used at 30 μg/mL, 200 μM, and 1 μM concentrations, respectively. Alpha-factor (Genscript) was used at 1.43 μM, unless indicated.

Microfluidic Device

The microfluidic device was constructed by soft lithography, and is composed of a cover glass and two layers of PDMS (Sylgard 184; Dow Corning), produced by replica molding from SU-8 fabricated wafers. Two wafers with the replicated microstructures were made by photolithography using negative photoresists (SU-8; Microchem Corp.). One is for the "control" PDMS layer to impose compressive mechanical stress with SU-8 3050 (height = 100 μm) (Fig. S1*A*), and the other one is for the "fluidics" PDMS layer to provide fluids (cell suspension, media, and reagent) and to load cells beneath the micro patch pad array with SU-8 10 (height = 15 μm) (Fig. S1*B*) and SU-8 3025 (height = 30 μm) (Fig. S1*C*), respectively. The dimensions of the device are presented in Fig. S1, and the design file will be provided upon request. After fabrication on the wafers, the surfaces were salinized to enhance detachment of PDMS during replica molding. For salinization, the wafers were placed into a desiccator with 100 μL of 1H,1H,2H,2H-perfluorodecyltrichlorosilane (ABCR GmbH) and incubated 24 h in the vacuumed environment. PDMS replication followed established procedures (2).

For PDMS replication, the PDMS base and curing agent were thoroughly mixed in a 1:10 wt/wt ratio, and degassed in a vacuum chamber to remove air bubbles. To fabricate the PDMS "control layer," the degassed mixture was poured onto the SU-8 master mold and cured on a hot plate (95 °C for 1 h and 135 °C for 1 h). The cured PDMS was then carefully peeled off the mold, and the air holes were punched using a biopsy punch. To construct the thin "fluidics layer," the degassed PDMS mixture was spread on the wafer using a spin coater (spinning speed 850 rpm) and cured on a hot plate (95 °C for 30 min). After PDMS-curing both layers, their surfaces were subjected to UV irradiation (UV Ozone cleaner PSD-UVT; Novascan) for 6 min to activate the surface for covalent bonding. Immediately after the activation, the two PDMS layers were aligned and incubated overnight in a hot oven at 80 °C. The bonded PDMS layers were cut and attached to cover glass by the same process of UV irradiation and incubation in a hot oven. Finally, the plastic well (bottomless well strips; Evergreen Scientific) was glued on top of the PDMS–glass hybrid device such that the well makes a junction between the compressed airflow and the PDMS–glass device (2). The compressed airflow was applied via a microfluidic pressure controller (ONIX Cellasic; Millipore), which is established by the diaphragm pump, the compressed air tank, the electronic pressure regulator, and the solenoid valves. The magnitude and duration of compressive pressure was controlled using software provided by the manufacturer.

We estimated the cell stiffness (Young's modulus G = 0.09 MPa to 0.57 MPa) according to a recent publication (3) by considering the change in the deformation rate of the height direction, which is defined as the correlation $P = G \times h/h0$ (P: pressure, G, Young's modulus; h, height of compressed cell; and $h0$, initial height of cell). While AFM measurements directly measure force, and are thus more accurate, our stiffness values are comparable to or slightly lower than previous AFM studies (G = 0.49 MPa) (4). However, we note that our method provides the opportunity to perform live-cell measurements, which is crucial for investigating cell signaling networks.

Live-Cell Microscopy and Image Analysis

For live-cell microscopy, budding yeast cells were grown overnight to saturation and then allowed to resume exponential growth by incubation for ∼5 h at 30 °C after diluting the culture 100-fold into fresh growth medium (Synthetic Defined Media with 2% glucose, $OD_{600} \approx 0.05$). To attach yeast cells in the PDMS device, the glass surface was coated for 10 min to 30 min with Con A (1 mg/mL; Sigma Aldrich) in PBS (1 mg/mL). The microfluidic chamber was rinsed with cell culture medium before loading the cells.

The microfluidic device was mounted on the stage of an inverted Nikon Eclipse Ti microscope, equipped with a hardware-based automated focusing system (Perfect Focus System). The device was placed into an incubation chamber set to 30 °C. Images were acquired with 60× oil objectives, and the appropriate excitation and emission filters were controlled using micromanager open source software (5). A motorized XY stage and piezo drive was used to acquire z stacks and multiple fields of view per time point. Where indicated, images were deconvolved using the Huygens software (Scientific Volume Imaging) and projected using maximum intensity projection. Raw data supporting the findings of this study are available from the authors upon request.

Automated image analysis was performed using YeastQuant software on raw images (6) running in Matlab. The relative nuclear relocalization of the translocation reporters and the Pkc1–GFP translocation to the plasma membrane was quantified as mean normalized SD of 75% bright pixel intensity in a segmented cell and membrane cell, respectively. Actin was stained using rhodamine-labeled phallodin. To quantify actin patches, deconvolved images were converted into binary images by manual application of the threshold function to ensure proper foci segmentation. The number of foci was counted by the image process function in ImageJ (Wayne Rasband, National Institutes of Health, Bethesda, MD). For viability assays, a 0.025% trypan blue solution was used to stain dead cells, which were then counted manually.

For statistical analysis, a nonpaired, two-tailed t test in Microsoft Excel was performed when indicated. The level of statistical significance is represented as follows: not significant (n.s.) = $P > 0.05$; $^{*}P \leq 0.05$; $^{**}P \leq 0.01$; $^{***}P \leq 0.001$.

1. Brachmann CB, et al. (1998) Designer deletion strains derived from *Saccharomyces cerevisiae* S288C: A useful set of strains and plasmids for PCR-mediated gene disruption and other applications. *Yeast* 14:115–132.
2. Lee SS, et al. (2012) Quantitative and dynamic assay of single cell chemotaxis. *Integr Biol* 4:381–390.
3. Yokokura T, Nakashima Y, Yonemoto Y, Hikichi Y, Nakanishi Y (2017) Method for measuring Young's modulus of cells using a cell compression microdevice. *Int J Eng Sci* 114:41–48.
4. Pillet F, et al. (2014) Uncovering by atomic force microscopy of an original circular structure at the yeast cell surface in response to heat shock. *BMC Biol* 12:6.
5. Edelstein AD, et al. (2014) Advanced methods of microscope control using μManager software. *J Biol Methods* 1:e10.
6. Pelet S, Dechant R, Lee SS, van Drogen F, Peter M (2012) An integrated image analysis platform to quantify signal transduction in single cells. *Integr Biol* 4: 1274–1282.

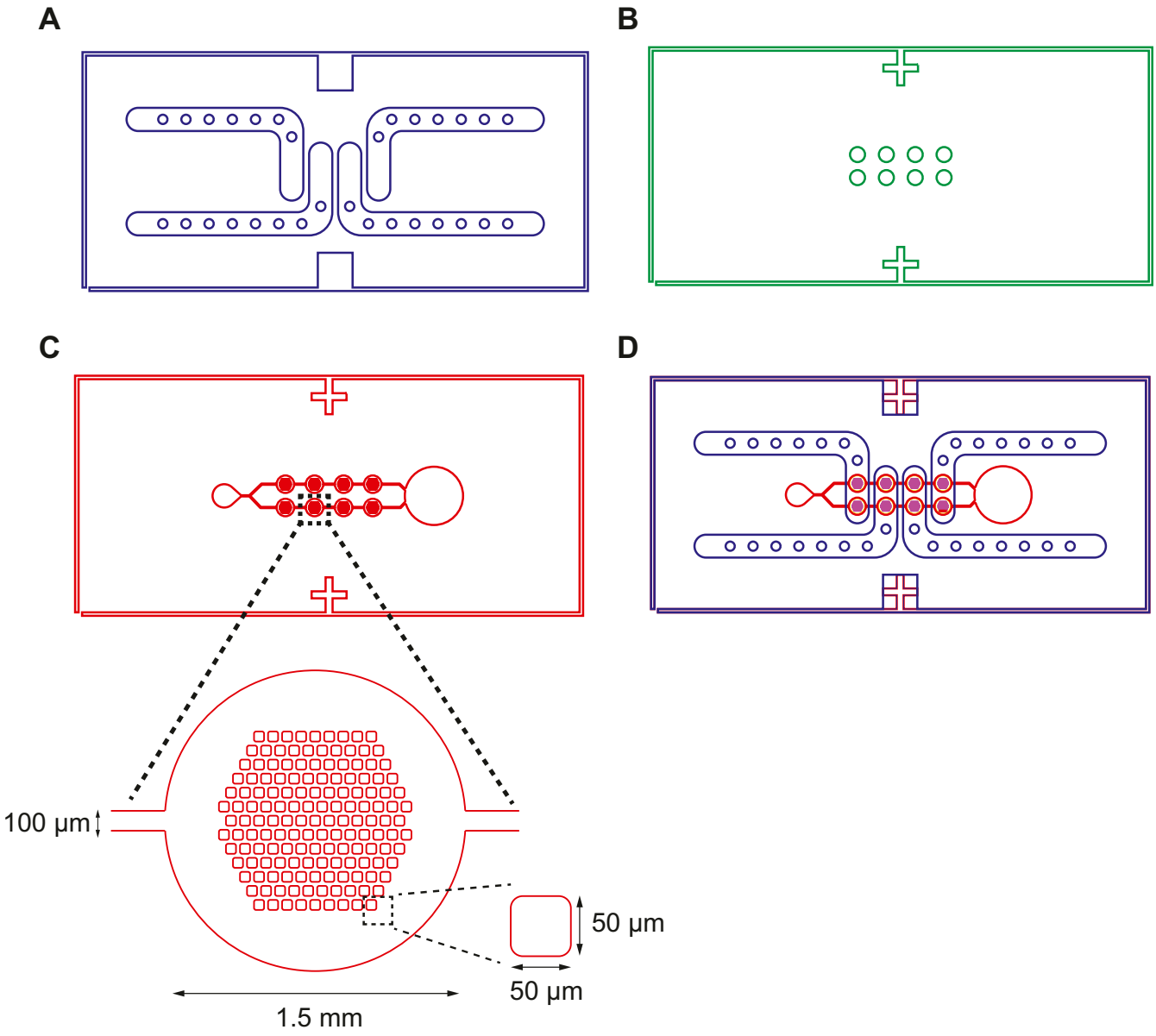

Fig. S1. Drawing for wafer fabrication of the microfluidics device to trigger compressive mechanostress. Two wafers were constructed. One is for the control PDMS layer to impose compressive mechanical stress, and the other one is for the fluidics PDMS layer to provide fluids (media and reagents) and to load cells in suspension beneath the micro patch pad array. The CAD drawing file will be made available upon request. (*A*) Drawing of the control layer (height = 100 μm). (*B* and *C*) Drawing of the fluidics layer. (*B*) Drawing of the gap between the micro patch pad array and the coverslip (height = 15 μm). (*C*) Drawing of the micro patch pad array (height = 30 μm). (*D*) Aligned drawing of all layers.

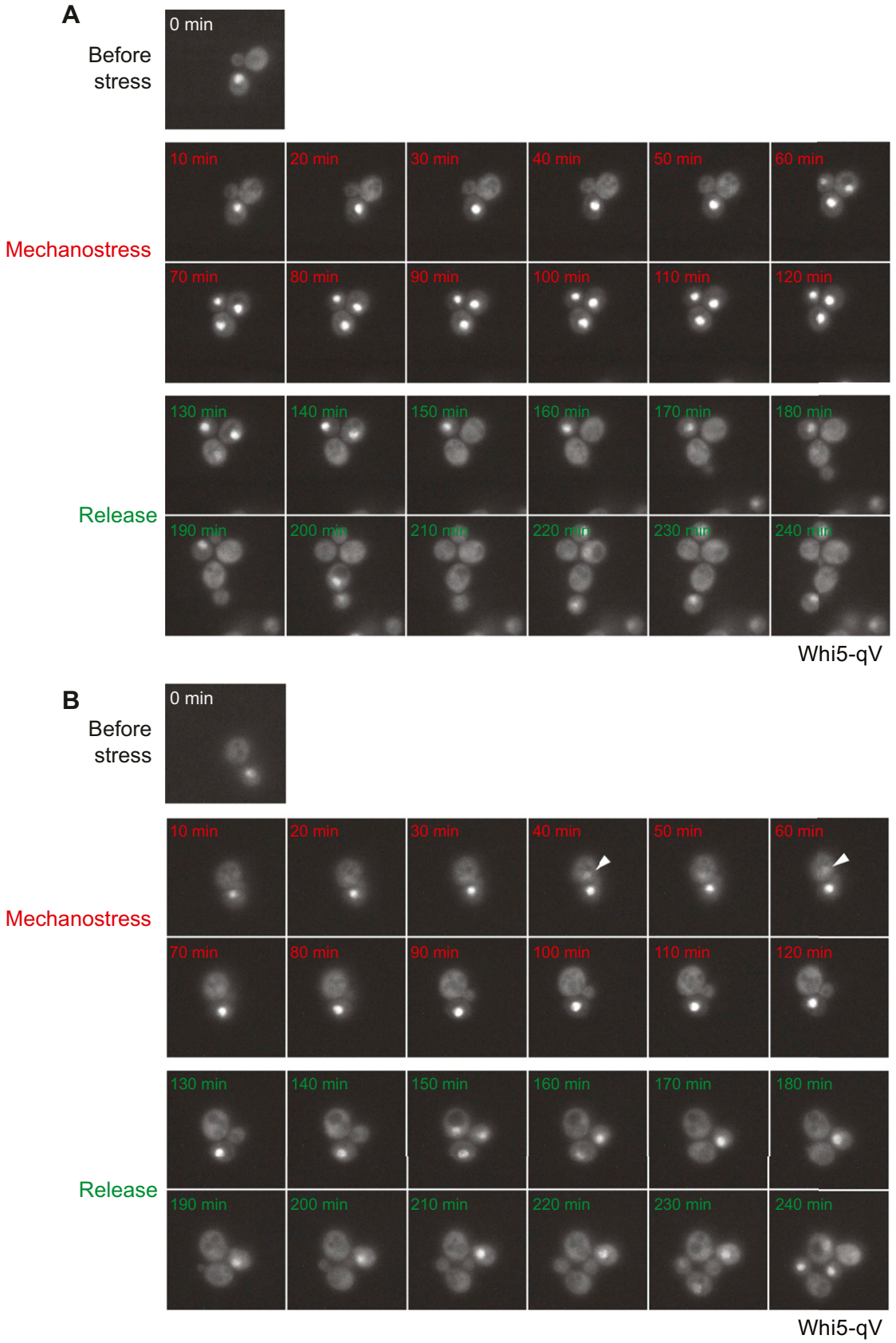

Fig. S2. Dynamics of Whi5-qv under mechanostress conditions. Exponentially growing cells were subjected to mechanostress for 2 h (Mechanostress, red time points) and then released for another 2 h (Release, green time points). Dynamics of Whi5-qV was monitored by live-cell imaging. (*A*) Example of cells that progress through the cell cycle before arresting in G1 with nuclear Whi5-qV. (*B*) Example of a cell that accumulates Whi5-qV in the nucleus despite the presence of a small bud (white arrowhead). Images are taken with objective lens (magnification: *A* and *B*, 60×).

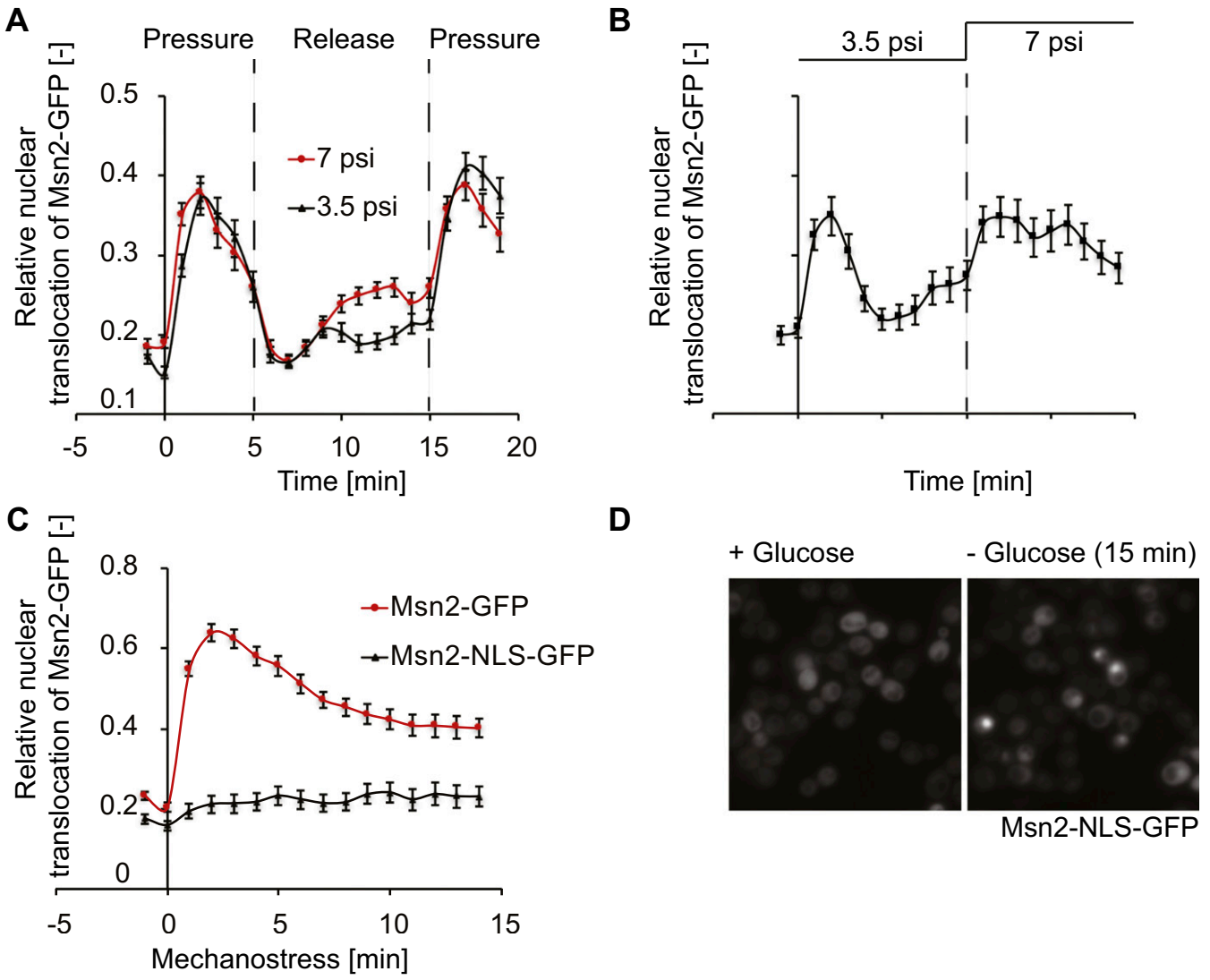

Fig. S3. Characterization of microfluidic device used for triggering compressive mechanical stress conditions. (*A* and *B*) Reversibility of the microfluidic platform as demonstrated by the Msn2−GFP reporter. Msn2−GFP was expressed from a plasmid under control of the constitutive *ADH* promoter. Cells were grown to midlog phase, and compressive mechanostress was applied (*A*) in pulse or (*B*) stepwise, with indicated pressures (pounds per square inch). Images were acquired in a z stack and analyzed from maximum intensity projections. Nuclear shuttling of Msn2−GFP was quantified based on the mean normalized SD of the 80% brightest pixels in each individual cell. The error bars indicate SE of mean of at least 45 cells in each experiment. (*C*) Mechanostress does not alter the activity of PKA. Exponentially growing cells expressing from the *ADH* promoter either wild-type Msn2-GFP (red dots) or an Msn2-GFP variant that responds exclusively to PKA (Msn2-NLS-GFP; black triangles) (1) were exposed to compressive mechanostress, and nuclear relocation was monitored for 15 min. The error bars indicate SE of mean with at least 50 cells in each experiment. (*D*) Exponentially growing cells harboring a plasmid expressing Msn2-NLS-GFP from the *ADH* promoter were glucose-starved for 15 min before imaging. Note that, in contrast to compressive stress (Fig. S2*C*), Msn2-NLS-GFP translocates into the nucleus upon glucose starvation, indicating lowered PKA activity. Images are taken with objective lens (magnification: 60×).

1. Görner W, et al. (2002) Acute glucose starvation activates the nuclear localization signal of a stress-specific yeast transcription factor. *EMBO J* 21:135–144.

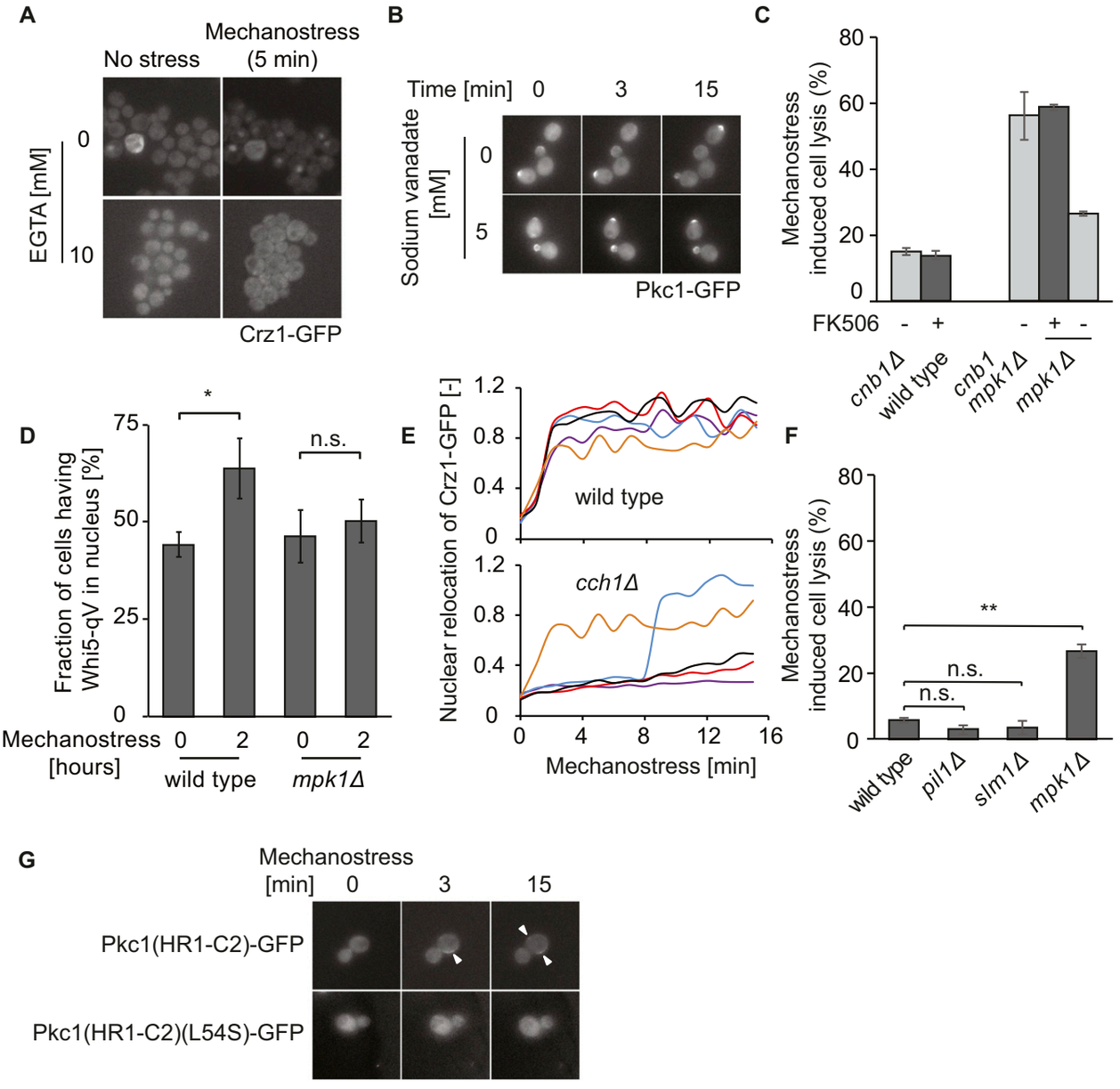

Fig. S4. Role of calcium signaling, CWI pathway and eisosomes in mechanostress responses. (*A*) Influx of extracellular calcium from the medium in response to compressive mechanostress. Exponentially growing cells expressing Crz1-GFP from endogenous locus were buffered with the indicated concentration of EGTA, and compressive mechano-stress was applied. Images were acquired in a z stack, and maximum intensity projected representative images showing nuclear translocation of Crz1-GFP after 5 min of stress (7 psi) are depicted. (*B*) Dynamics of Pkc1-GFP during sodium vanadate-mediated cell wall stress. Exponentially growing cells expressing Pkc1-GFP were monitored at the times indicated (minutes) after addition of the indicated concentration of sodium vanadate to activate general cell wall stress. Note that, in contrast to compressive mechanostress (Fig. 2*C*), Pkc1-GFP remains predominantly at sites of polarized growth upon general cell wall stress caused by sodium vanadate. (*C*) Treatment of cells with FK506 mimics deletion of *CNB1*. Compressive mechanostress was applied to exponentially growing cells of the indicated strains with or without treatment with FK506. Both stressed and nonstressed cells were incubated with 0.025% trypan blue for 15 min. The total cell number and trypan blue-stained cells were counted manually, and mechanostress-induced cell lysis was determined by subtracting the cell lysis in the control cell chamber from cell lysis in the chamber where mechanostress was applied. The error bars indicate SEM of at least two experiments, each with more than 500 cells counted. (*D*) Activation of Mpk1 by mechanostress leads to cell cycle arrest with nuclear Whi5-qV. Mechanostress was applied for 2 h to exponentially growing wild-type or *mpk1Δ* cells, and the fraction of cells with nuclear Whi5-qV was counted. The error bars indicate the SEM of five independent experiments. (*E*) Single-cell traces of Crz1-GFP nuclear relocation upon mechanostress. The graphs show nuclear relocation dynamics of five cells for wild-type and cch1Δ strains when subjected to mechanostress. The mean of such single-cell traces is shown in Fig. 3*B*. (*F*) Eisosomes are not required for compressive stress signaling. Mechanostress-induced cell lysis in wild-type, *mpk1Δ* control cells or cells lacking the indicated eisosome components was quantified as described in *C*. (*G*) Active Rho1 is recruited to the plasma membrane upon compressive mechanostress. Membrane recruitment of active Rho1 was analyzed using a specific biosensor. Cells expressing a Pkc1 fragment that specifically binds GTP-bound Rho1 [Pkc1(HR1-C2)-GFP, *Upper*] or its nonbinding control variant [Pkc1(HR1-C2) (L54S)-GFP, *Lower*] were grown to midlog phase before mechanostress (7 psi) was applied for the indicated time (minutes) (1). The depicted images are maximum intensity projections of z stacks. Note that the active biosensor is rapidly recruited to the plasma membrane (arrow heads), confirming activation of Rho1 upon mechanostress. Student's *t* test was performed between the arrays of data, and results are indicated in the figure (n.s., nonsignificant; $*P < 0.05$; $**P < 0.01$). Images are taken with objective lens (magnification: *A*, *B*, and *G*, 60×).

1. Kono K, Saeki Y, Yoshida S, Tanaka K, Pellman D (2012) Proteasomal degradation resolves competition between cell polarization and cellular wound healing. *Cell* 150:151–164.

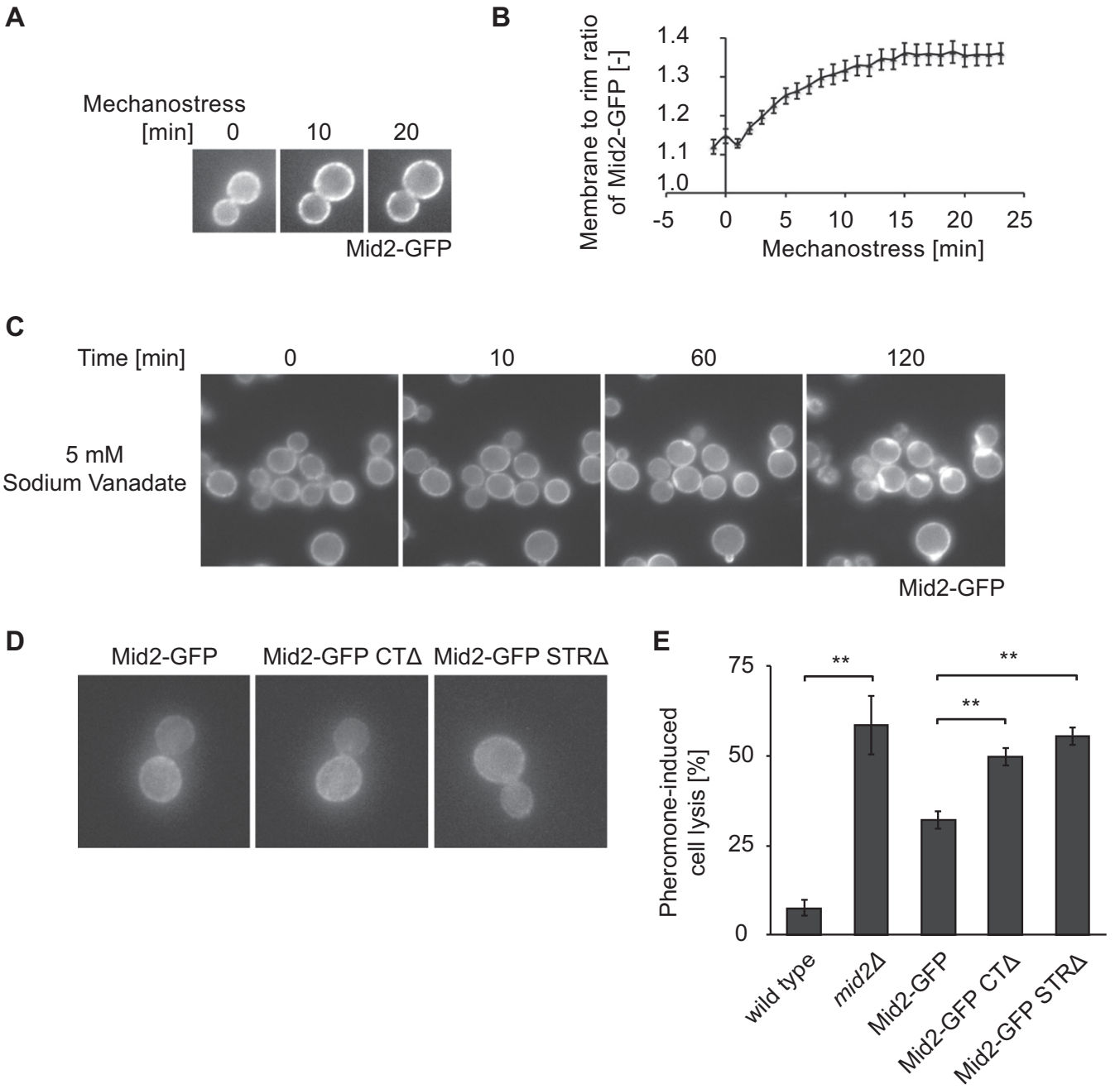

Fig. S5. Characterization of the Mid2 mechanosensor. (*A*) The localization of GFP-tagged Mid2 (Mid2-GFP) was analyzed by fluorescent microscopy in wild-type cells exposed to mechanostress for the times indicated (minutes). (*B*) The ratio of Mid2-GFP intensity at the plasma membrane compared with cytosolic rim localization was quantified. Error bars indicate the SEM for 28 analyzed cells. (*C*) Exponentially growing cells expressing Mid2-GFP were monitored at the times indicated (minutes) after addition of the indicated concentration of sodium vanadate to activate general cell wall stress. Note that, in contrast to compressive mechanostress (Fig. 3*E*), Mid2−GFP enriches at sites of polarized growth and bud neck after treatment with sodium vanadate-mediated cell wall stress. (*D*) Expression and localization of wild type and the indicated Mid2-GFP mutants. Cells expressing from its endogenous promoter Mid2-GFP, Mid2 lacking its C terminus CT (amino acids 256 to 376, Mid2−GFP CTΔ) or its N-terminal STR (amino acids 30 to 197, Mid2−GFP STRΔ) domain were grown until midlog phase, and representative maximum intensity projection images are shown. (*E*) Wild-type, *mid2Δ*, and *mid2Δ* cells expressing from the endogenous promoter Mid2-GFP, Mid2-GFP CTΔ, or Mid2-GFP STRΔ were exposed to a high concentration of mating pheromones (11.5 μM alpha-factor), and cell lysis was visualized after 4 h by trypan blue staining. The total cell number and trypan blue-stained cells were counted manually, and pheromone-induced cell lysis was plotted as percentage of the total cell number. The error bars indicate SEM of at least two experiments, each with more than 500 cells counted. Note that the extracellular Mid2 domain with spring-like properties as well as its intracellular tail are required for its function in vivo. Student's *t* test was performed between the arrays of data and indicated in the figure (**$P < 0.01$). Images are taken with objective lens (magnification: *A*, *C*, and *D*, 60×).

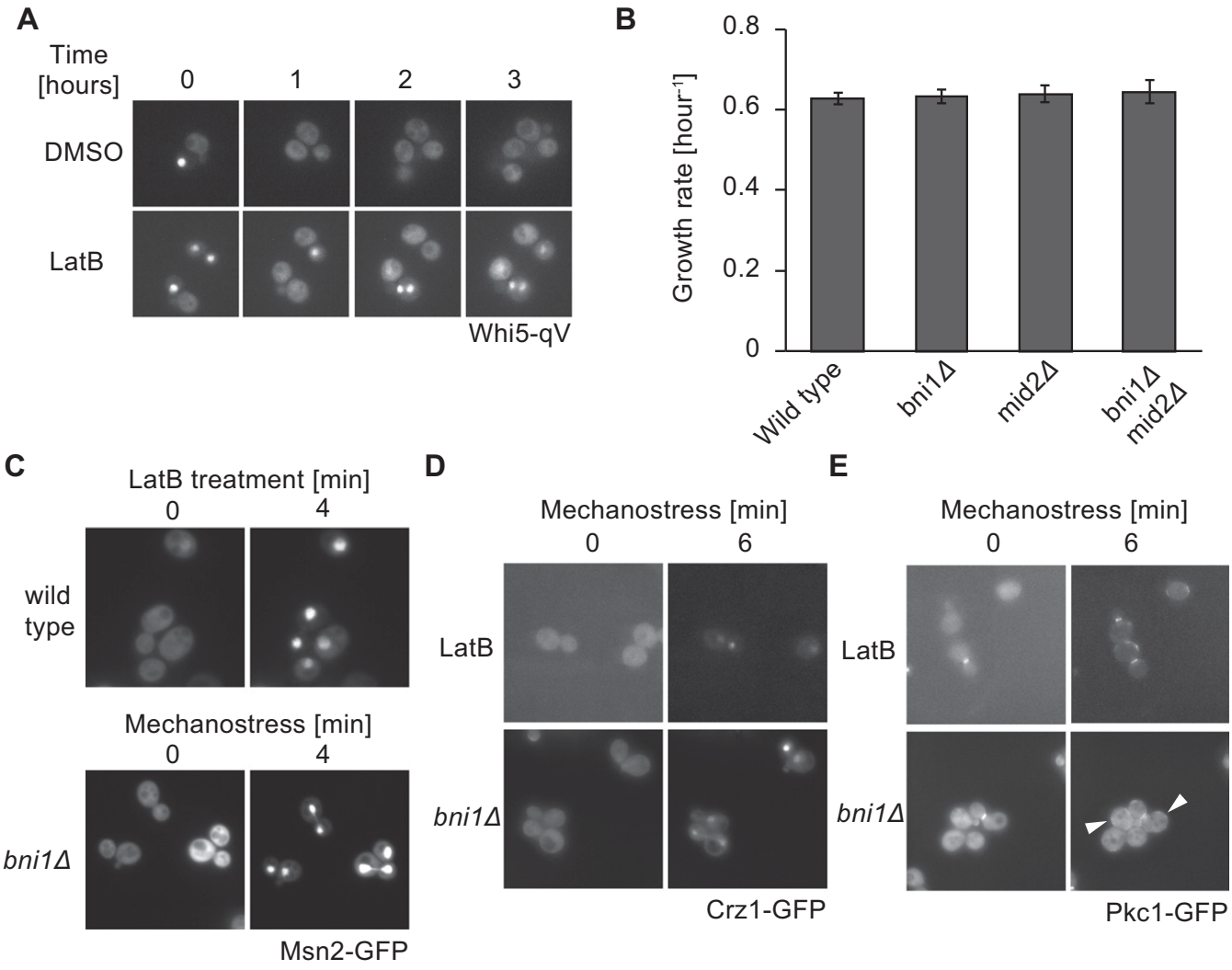

Fig. S6. Mechanostress responses in cells inhibited for actin polarization. (*A*) Cells expressing Whi5-qV were treated with DMSO or LatB, and Whi5-qV dynamics were monitored for 3 h by live-cell imaging. (*B*) The growth rate of the indicated strains was compared in rich medium (YPD). (*C*) Msn2-GFP dynamics in wild-type cells when treated with LatB alone (*Upper*) and in *bni1Δ* cells when subjected to mechanostress (*Lower*). Note that LatB treatment triggered nuclear relocation of Msn2-GFP, and thus mechanostress-induced dynamics of Msn2-GFP was not monitored in LatB-treated cells. Msn2-GFP was expressed from a centromeric plasmid under the control of the *ADH* promoter. (*D* and *E*) Mechanostress-induced dynamics of (*D*) Crz1-GFP and (*E*) Pkc1-GFP were measured in LatB-treated wild-type (*Upper*) or *bni1Δ* cells (*Lower*). While both fluorescently tagged proteins were expressed from the endogenous locus in wild-type cells, they were expressed from centromeric plasmids under the control of *ADH* promoter in *bni1Δ* cells. Note that LatB treatment or *BNI1* deletion does not interfere with mechanostress-induced nuclear translocation of Crz1-GFP or plasma membrane recruitment of Pkc1-GFP. Images are taken with objective lens (magnification: *A* and *C*–*E*, 60×).

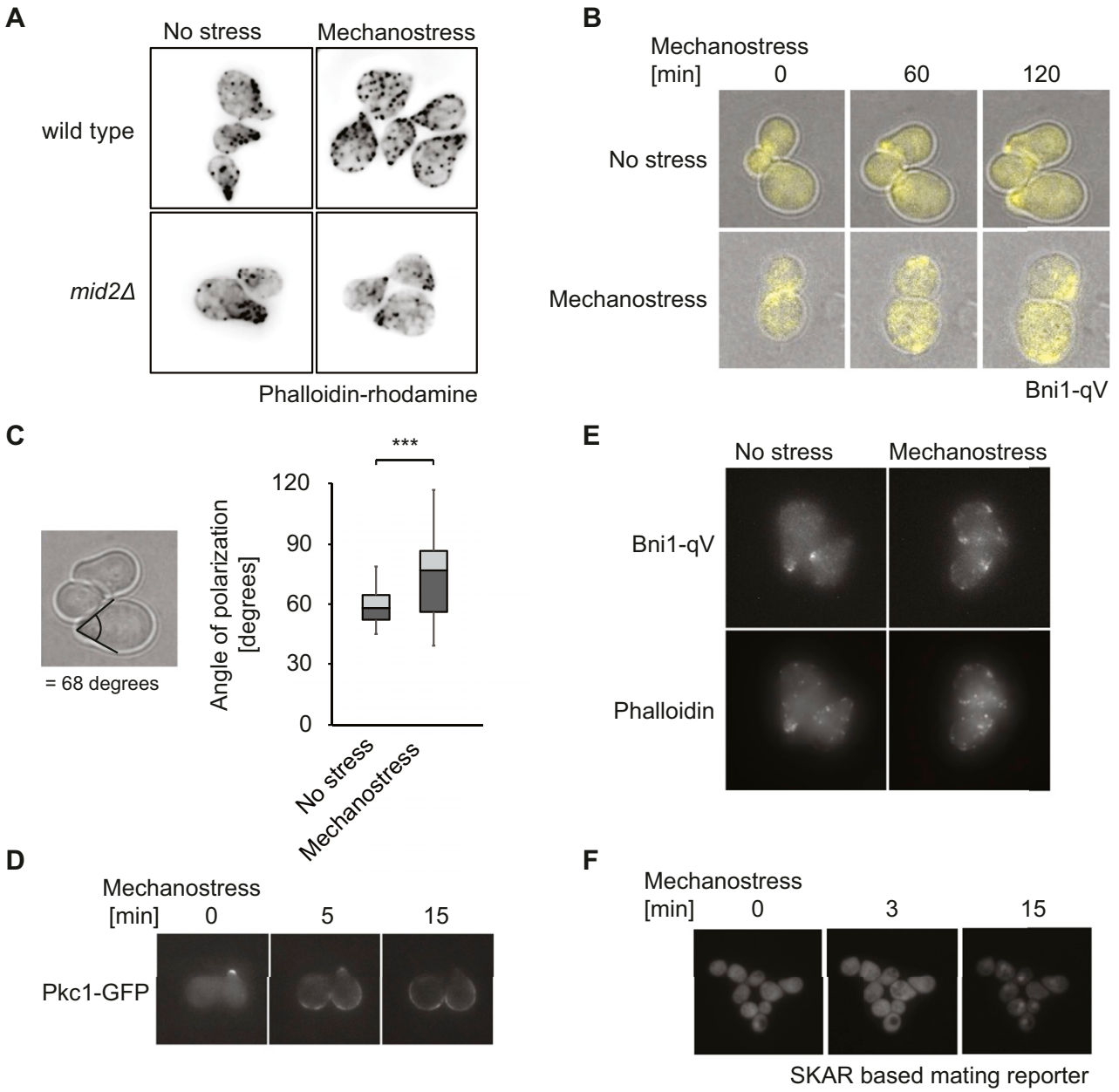

Fig. S7. Application of mechanostress reverses pheromone-induced cell polarization by inhibiting Fus3. (*A*) Mid2-dependent reorganization of the actin cytoskeleton upon compressive mechanostress. Exponentially growing wild-type and *mid2Δ* cells were treated with 1.43 μM alpha-factor for 90 min, and mechanostress was applied for 30 min. The actin cytoskeleton was stained with rhodamine phalloidin. Deconvolved images are shown, with quantification shown in Fig. 5*A*. (*B*) Simultaneous application of mechanostress and pheromone prevents polarized localization of Bni1. Cells expressing Bni1-qV from the endogenous locus were simultaneously exposed to alpha-factor and mechanostress, and the localization of Bni1-qV followed by live imaging is shown at the indicated times (minutes). (*C*) Measuring the angle of pheromone-induced polarization of cells with and without exposure to mechanostress. Cell polarization was quantified by measuring the angle of the shmoo after 2 h of mechanostress and alpha-factor treatment. Student's *t* test was performed between the arrays of data indicated in the figure (***$P < 0.01$). (*D*) Redistribution of Pkc1-GFP from shmoo tips to the plasma membrane upon mechanostress. Cells were treated with alpha-factor for 90 min, mechanostress (7 psi) was applied for the times indicated (minutes), and membrane enrichment of Pkc1-GFP was monitored microscopically. (*E*) Actin redistribution follows formin Bni1. Cells expressing Bni1-qV from the endogenous locus were treated with alpha-factor for 90 min, and mechanostress was applied for 30 min. After mechanostress, cells were stained for actin using rhodamine phalloidin and subsequently imaged for both actin and Bni1-qV. (*F*) Mechanostress inhibits Fus3 activity. The activity of Fus3 was monitored using the SKAR sensor (1). Cells expressing the SKAR sensor were exposed to alpha-factor for 30 min before compressive mechanostress (7 psi) was applied for the times indicated (minutes). Maximum intensity projected representative images are shown. Note that Fus3 activity is rapidly inhibited, indicated by the nuclear accumulation of the SKAR biosensor upon mechanostress. Images are taken with objective lens (magnification: *A* and *E*, 100×; *B–D* and *F*, 60×).

1. Durandau E, Aymoz D, Pelet S (2015) Dynamic single cell measurements of kinase activity by synthetic kinase activity relocation sensors. *BMC Biol* 13:55.

Table S1. Plasmids used in this study

Plasmid	Genotype	Backbone	Source
pRM1	Msn2-GFP	pRS315	(1)
pRM2	Msn2-GFP-NLS	pRS315	(1)
pRM17	PB2729: Pkc1(HR1-C2)-GFP	pRS316	(2)
pRM18	PB2997: Pkc1(HR1-C2)(L54S)-GFP	pRS316	(2)
pRM24	Pkc1-GFP	pRS415	This study
pRM25	Crz1-GFP	pRS415	This study

1. Görner W, et al. (2002) Acute glucose starvation activates the nuclear localization signal of a stress-specific yeast transcription factor. *EMBO J* 21:135–144.
2. Kono K, Saeki Y, Yoshida S, Tanaka K, Pellman D (2012) Proteasomal degradation resolves competition between cell polarization and cellular wound healing. *Cell* 150:151–164.

Table S2. Yeast strains used in this study

Strain ID	Genotype	Source
BY4741	*MATa; his3Δ1, leu2Δ0, met15Δ0, ura3Δ0*	OpenBiosystems
yJT191	[BY4741] *MID1::kanMX*	This study
yJT197	[BY4741] *MID2::kanMX*	This study
yJT195	[BY4741] *MID1::kanMX MID2::kanMX*	This study
yRM181	[BY4741] *MID1::kanMX CCH1::kanMX*	This study
yRM202	[BY4741] *MPK1::kanMX*	This study
yJT284	[BY4741] *CNB1::kanMX*	This study
yRM199	[BY4741] *MPK1::kanMX CNB1::kanMX*	This study
yRM7	[BY4741] *MSN2::kanMX*	This study
yRM190	[BY4741] *BNI1::kanMX*	This study
yRM219	[BY4741] *BNI1::kanMX MID2::kanMX*	This study
yJT280	[BY4741] *PIL1::kanMX*	This study
yJT282	[BY4741] *SLM1::kanMX*	This study
yRM183	[BY4741] *BNI1:qVenus::URA3 TMD-dCherry::LEU2*	(1)
yRM187	[yRM183] *MID2::kanMx*	This study
yRM193	[yRM183] *MPK1::kanMx*	This study
yRM196	[yRM183] CNB1*::kanMx*	This study
yRM230	[yRM183] *FUS3::fus3-as1-URA3*	This study
yRM120	[BY4741] *PKC1::PKC1-GFP-HIS3 TMD-dCherry::URA3*	This study
yRM124	[yRM120] *MID2::kanMx*	This study
yRM128	[yRM120] *WSC1::kanMx*	This study
yRM101	[yRM120] *MID1::kanMx*	This study
yFD365	[BY4741] *CRZ1::CRZ1-GFP-HIS3*	(2)
yFD367	[yFD365] *MID1::kanMx*	This study
yFD368	[yFD365] *CCH1::kanMx*	This study
yJT212	[yFD365] *MID2::kanMx*	This study
yRM229	[BY4741] *RPL9A::RPL9A-GFP-HIS3*	(2)
yRM140	[BY4741] *Whi5-qV::URA3*	This study
yRM147	[yRM140] *MPK1:: kanMx*	This study
yFD385	[BY4741] *MID2::MID2-GFP-HIS3*	(2)
yFD386	[BY4741] *ROM2::ROM2-GFP-HIS3*	(2)
yRM207	[BY4741] *CDC19::CDC19-GFP-HIS3*	(2)
yRM232	[yJT197] *LEU2::pRS305-Mid2-GFP*	This study
yRM236	[yJT197] *LEU2::pRS305-Mid2-GFP* CTΔ	This study
yRM238	[yJT197] *LEU2::pRS305-Mid2-GFP* STRΔ	This study

1. Hegemann B, et al. (2015) A cellular system for spatial signal decoding in chemical gradients. *Dev Cell* 35:458–470.
2. Huh WK, et al. (2003) Global analysis of protein localization in budding yeast. *Nature* 425:686–691.

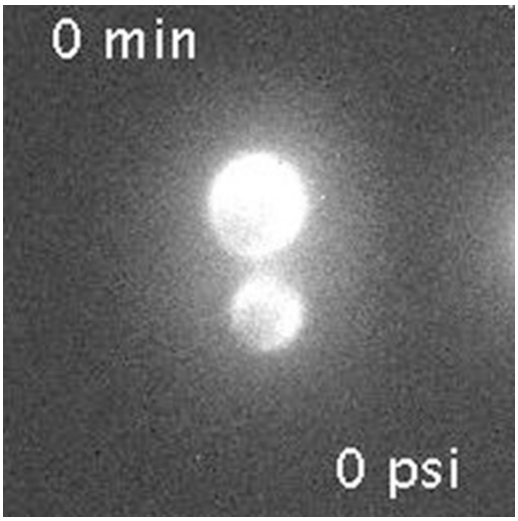

Movie S1. A microfluidic device that delivers compressive stress with variable pressure elicits a reversible cellular response. Yeast cells expressing fluorescently tagged Rpl9A (Rpl9A-GFP) were grown to midlog phase. Pressure (7 psi) was applied in the sequence indicated in the movie. A z stack of images was acquired every 2 min, and a representative movie was created by compiling maximum intensity projection images for each time point. Note that the contact area of cells with the cover glass increases in size when compressive stress is applied. Cells rapidly return to their original size after release of pressure. Quantification of the movie is shown in Fig. 1*E*.

Movie S1

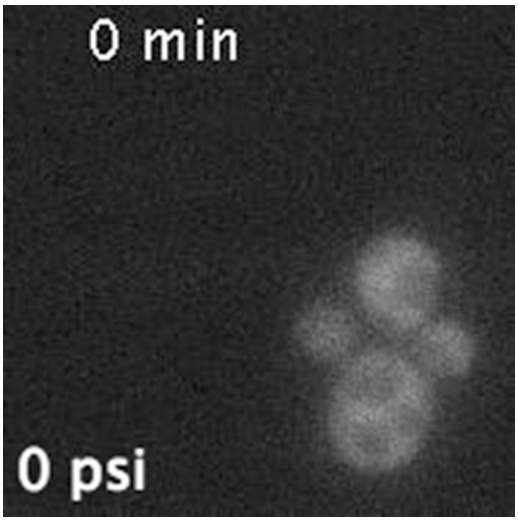

Movie S2. Dynamics of fluorescently tagged Whi5 during 4 h of cell growth in the microfluidic device. Exponentially growing cells expressing Whi5-qV were loaded in a microfluidic chip and imaged for 4 h to monitor Whi5 dynamics. Time interval is 10 min per frame. Representative still images are shown in Fig. 1*G*.

Movie S2

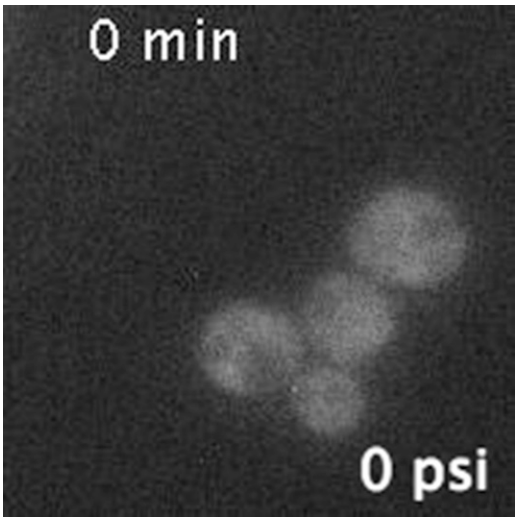

Movie S3. Cells arrest with Whi5 in the nucleus under mechanostress, but restart normally after release of stress. Exponentially growing cells expressing Whi5-qV were loaded in a microfluidic chip and pressure was applied in the sequence indicated in the movie. The dynamics of Whi5 was monitored every 10 min for 4 h. Note that, in contrast to Movie S2 showing Whi5-qV dynamics in absence of compressive stress, this movie shows cell cycle arrest and Whi5-qV accumulating in the nucleus when pressure (7 psi) was applied. Representative still images are shown in Fig. 1*G*.

Movie S3

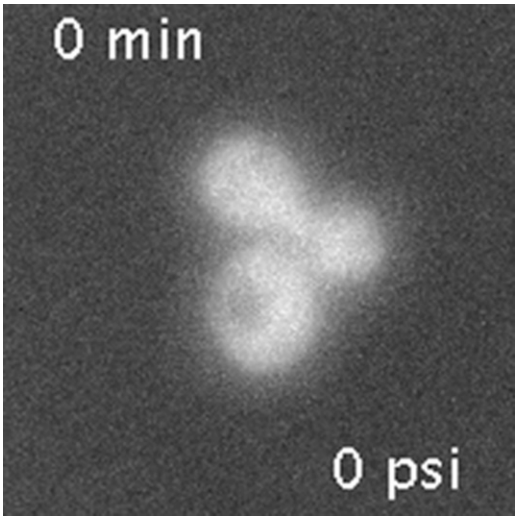

Movie S4. Dynamics of Crz1 upon application of compressive mechanostress. Mechanostress (7 psi) was applied to cells expressing Crz1-GFP. Images were acquired in z stacks every minute for 15 min. The movie is the compilation of maximum intensity projected images. Quantification of the movie is shown in Fig. 2*B*, *Lower*.

Movie S4

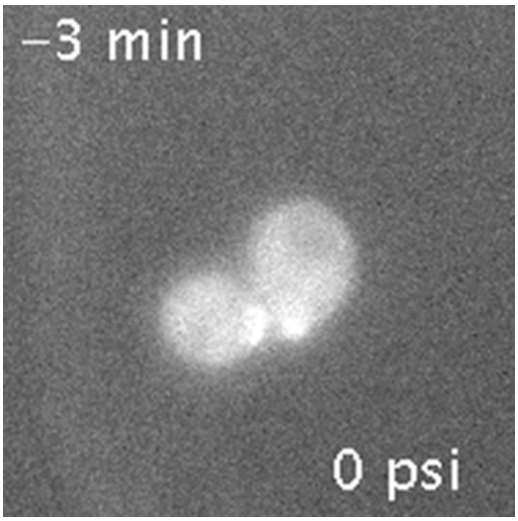

Movie S5. Dynamics of Pkc1 upon application of mechanostress. Mechanostress (7 psi) was applied for 15 min to exponentially growing cells expressing Pkc1-GFP. Pkc1-GFP dynamics was monitored every 3 min in several z planes. A representative movie was created using maximum intensity projected images for each time point. Quantification of the movie is shown in Fig. 2*C*, *Lower*.

Movie S5